PHYSOR 2004 -The Physics of Fuel Cycles and Advanced Nuclear Systems: Global Developments
Chicago, Illinois, April 25-29, 2004, on CD-ROM, American Nuclear Society, Lagrange Park, IL. (2004)

Consistent Comparison of Monte Carlo and Whole-Core Transport Solutions for Cores with Thermal Feedback

Han Gyu Joo[*1], Jin Young Cho[1], Kyo Youn Kim[1], Moon Hee Chang[1]
Beom Seok Han[2] and Chang Hyo Kim[2]
[1]*Korea Atomic Energy Research Institute, Yuseong, Daejeon 305-600, Korea*
[2]*Seoul National University, San 56-1, Shillim-dong, Seoul, 159-741, Korea*

For systematic and consistent comparison of Monte Carlo and whole-core transport solutions in various core states including power generating conditions, a test problem set that spans from two-dimensional uniform temperature pin cell problems to three-dimensional core problems involving thermal feedback is solved by a continuous energy Monte Carlo code MCCARD and a multigroup whole-core transport code DeCART. The neutron spectra, k-effective, pin-wise power distribution, fuel temperature distribution, and Doppler coefficients obtained from the two solutions are compared taking the MCCARD solution as the reference. For the uniform temperature problems, excellent agreement between the two solutions is observed in every solution aspect. The pin power distribution error is less than 1% and the k-effective error is within 100 pcm in most cases. For the problems with thermal feedback, the discrepancy becomes larger, yet within the tolerable range. In the hot-full-power minicore calculation, a maximum of 3.7% error in the radial pin power distribution and the k-effective error of about 260 pcm are observed. Through this comparison, it is demonstrated that accurate multigroup direct whole-core calculations are possible even at power generating conditions with a much less computing time than the corresponding Monte Carlo calculations.

KEYWORDS: Monte Carlo, Whole-Core Transport, Thermal Feedback, MCCARD, DeCART

1. Introduction

In order to be applicable for the analysis of actual core problems involving power generation, a whole-core transport code is required to have at least the following three major components: a transport solver, a multigroup macroscopic cross section generator, and a thermal/hydraulic (T/H) solver. These three components involve their own sources of error and the combined error appears in the final solution. Although the combined error is the most important one, it is desirable to isolate the sources of error to verify each component separately. In this regard, a consistent comparison of the solutions of a whole-core transport code with those of a Monte Carlo code is pursued in this work. The continuous energy Monte Carlo solutions obtained with conjugate thermal feedback are taken as the reference against which the multigroup whole-core transport solutions are compared.

DeCART[1] is a three-dimensional (3-D) whole-core code based on planar MOC solutions and the subgroup method for resonance treatment. The cross sections to be used in this code are obtained directly from a multigroup (e.g. 45 group) cross section library and subpin level regional temperatures are obtained in a power generating condition by a pin-wise

* Corresponding author, Tel. +82-42-868-2651, FAX +82-42-868-8990, E-mail: joohan@kaeri.re.kr

thermal-hydraulic solver. The regional temperatures are used to determine temperature dependent multigroup microscopic cross sections and also to update the moderator number densities. The transport calculation in DeCART is performed with the local macroscopic cross sections updated after each T/H calculation. The detailed methods employed in DeCART are presented in the companion paper[1]. In contrast to DeCART which is a multigroup deterministic code, MCCARD[2] is a continuous energy Monte Carlo code capable of incorporating thermal feedback. It has a simple T/H calculation module which generates ring-wise fuel temperature distributions and the axial coolant temperature profile in each closed flow channel. The continuous energy cross section data for the specific local temperature are obtained from a tabularized continuous energy cross section library that contains hundreds of continuous cross section data sets generated at different temperatures.

A test problem set was prepared for systematic and consistent comparison of the DeCART and MCCARD solutions. This problem set spans from the very basic two-dimensional (2-D) pin cell uniform temperature problems to the practical full power 3-D PWR core problems. Other problems includes 2-D assemblies and checkerboards, 2-D pin-cells with an intra-pellet temperature distribution, 3-D assembly at hot full power as well as hot zero power conditions. Normal uranium oxide and mixed oxide fuels are used for which isotopic number densities are specified. For uniform temperature cases, both room temperature (300K) and hot operating temperature (600K) are specified. For the problems with thermal hydraulic feedback, only the nominal power density and inlet flow conditions are specified and therefore the temperature distribution need to be calculated by the internal T/H solver of the code.

The multigroup cross section library to be used in DeCART is under development. Meantime, the HELIOS 45 group cross section library for Version 1.6 [3] is being used for the sake of code testing and performance evaluation. The HELIOS library was generated from the ENDF/B-VI files through the NJOY91.105[4]. In order to be consistent with the HELIOS cross section library as much as possible, the MCCARD continuous cross section data sets were generated from ENDF/B-VI as well using the ACER module of NJOY97.115[5].

In the following section, the MCCARD methods for generating the converged power and temperature distributions are briefly described. The test problem set specification is then given in Section 3. The comparison of the DeCART and MCCARD results are given in Section 4 for various test problems with increasing level of complexity. The run time performance of the two codes is also given in this section. Section 5 concludes the paper.

2. Methods for Thermal Feedback Calculation in MCCARD

Since the neutron flux distribution and the temperature distribution are nonlinearly coupled through the thermal feedback, it is necessary to employ repetitive alternate neutronics and T/H calculation scheme to obtain the converged flux and temperature distributions. In the iterative neutronics and T/H calculation scheme, it is expected that the initial stage flux and temperature distributions are far off from the converged ones and thus it is not necessary to converge fully the neutronics solutions during the initial stage of neutronics - T/H iteration. In this regard, a two-stage neutronics - T/H iteration scheme is employed in MCCARD.

In the first stage, the number of histories of the Monte Carlo (MC) neutronics calculation increases linearly with the iteration index. After each neutronics calculation, the T/H calculation is performed to update the thermal condition, namely, the fuel temperature, moderator density and temperature distributions. The convergence of the neutronic-T/H iteration is checked by monitoring the change in the fuel temperature. Specifically, the following two criteria are used:

$$\max\left|T_l^{i+1} - T_l^i\right| \le \Delta T \quad \text{or} \quad \max\left|T_l^{i+1} - T_l^i\right| \le \alpha\sigma_{R,est} \tag{1}$$

where i is the T/H calculation index and $\sigma_{R,est}$ is the estimated standard deviation of the fuel temperature which is inferred from the regional power density. The first criterion is to monitor the absolute change in the calculated fuel temperature and the second is to account for the uncertainty of the calculated fuel temperature. Normally, ΔT is set to 5K and the confidence level α is 3. The first stage calculation is terminated either the convergence criteria are met or the maximum number of histories is reached. In the second stage, the number of histories is set to the maximum number of histories and stays constant. The neutronics-T/H iteration in the second stage continues until the fuel temperature convergence criteria are met.

The T/H solver of MCCARD was not intended for a wide range of applications and thus was made very simple. The axial coolant temperature rise is calculated for each pin channel using the energy balance. Once the coolant bulk temperature is determined at each axial node, the wall temperature is determined using the heat flux and heat transfer coefficient determined from the Dittus-Boelter correlation. The fuel temperature profile within the pellet is determined using the heat resistance scheme in which the temperature dependent regional thermal conductivity is determined using the temperature available from the previous iteration. Normally, three annular regions are defined within the pellet and thus three volume average temperatures are used in the pellet region. The volume average temperature is used to determine which continuous energy cross section set to use. Hundreds of temperature dependent continuous energy cross section sets are given for each isotope and these are generated with temperature intervals of 5-10K to cover the operating temperature range. For a given region temperature, the nearest temperature set is chosen and no interpolation is employed. For moderator isotopes (H-1 and O-16), finer temperature intervals (1-2 K) are used.

The MCCARD cross section functionalization scheme is very simple and straightforward in that the code just picks up the nearest continuous energy cross data set for the given temperature of each cell. In order to ensure sufficient accuracy, however, the temperature interval of the continuous energy cross section sets should be kept small and this requirement leads to a large compilation of temperature dependent cross section data which have to be generated through a series of NJOY processing. When generating a continuous energy cross section data set for a given temperature, the RECONR, BROADR, and ACER modules of NJOY are used. In addition, the LEAPR and THERMR modules are also used for hydrogen to generate the thermal scattering data.

3. Test Problem Set

The test problem set consists of various test problems that were designed to examine different solution aspects of the DeCART code. For example, the simplest 2-D pin cell uniform temperature problem is designed to examine the accuracy of the cross section library while the checkerboard problem and the minicore problems are to examine the transport solver. The test problems were simplified as much as possible to avoid unnecessary complications and the specifications were made self sufficient. As a result, the helium gap and inter-assembly water gap are not modeled and isotopic number densities are given for each material composition. In the following, the geometrical, material, and thermal specifications are given.

3.1 Fuel Assembly and Core Specification

The fuel assembly is a 17x17 shortened length PWR fuel assembly. The cell pitch is 1.2660 cm and the active fuel stack height is 200 cm. The fuel rod consists of cladding and pellets whose outer diameters are 0.9518 and 0.8050 cm, respectively. There are 25 guide tubes whose inner and outer diameters are 1.1418 and 1.2260 cm, respectively. There are three fuel rod types: UOX, MOX, and Gadolina. The isotopic compositions of these fuels are given in Table 1 along with cladding and moderator compositions. These fuel rods constitute UOX, MOX, and GAD fuel assemblies. The configuration of the GAD fuel assembly is shown in Fig. 1 for the lower right quadrant along with the minicore configuration into which these fuel assemblies are loaded. In case of UOX and MOX assemblies, all 264 fuel rods are UOX or MOX rods, respectively. The nominal power generation rate of the assembly is 5.789574 Mw and the mass flow rate per assembly is 24.2421 Kg/sec. The system pressure is 15.0 MPa and the inlet temperature is 270°C. The thermal condition represents a 330 Mwth integral reactor loaded with 57 fuel assemblies defined above. For temperature dependent thermal conductivity for fuel pellet and clad, and the gap conductance data, the specification for the NEACRP PWR rod ejection problem set is used.

Table 1 Isotopic Composition of Assembly Constituent Materials

Material	Composition in Number Density, nuclides/barn-cm	Remark
UOX	U-235=1.11706e-3, U-238=2.14499e-2, O-16=4.51340e-2	UO2 4.95w/o
MOX	U-235=4.93159e-5, U-238=2.15926e-2, Pu-238=2.98094e-5 Pu-239=9.39680e-4, Pu-240=3.63448e-4, Pu-241=1.77917e-4 Pu-242=8.97093e-5, Am-241=1.73729e-5, O-16=4.65198e-2	MOX 7w/o
GAD	U-235=3.89929e-4, U-238=2.10005e-2, O-16=7.18084e-1 Gd-152=2.77081e-6, Gd-154=2.89111e-5, Gd-155=1.96414e-4 Gd-156=2.71519e-4, Gd-157=2.07708e-4, Gd-158=3.29772e-4 Gd-160=2.89926e-4	Gd_2O_3 4 w/o
CLAD	Cr-52=9.8698e-5, Fe-56=1.6952e-4, Zr-Nat.=4.2443e-2 Nb-93=8.4919e-6, Sn-118=1.8190e-4, Sn-120=2.4866e-4	
H2O300	H-1=6.6888720e-2, O-16=3.3444360e-2	@300K
H2O600	H-1=4.6822104e-2, O-16=2.3411052e-2	@600K

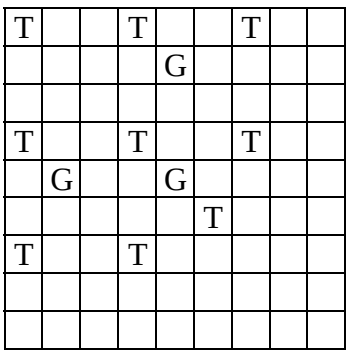

(G for Gadolinia; T for Guide Tube)

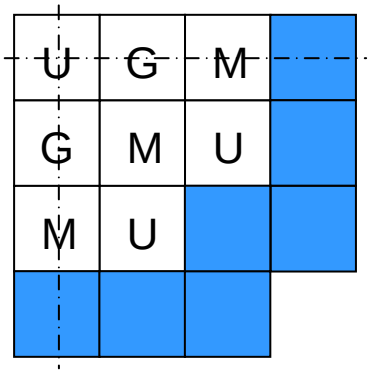

(U. M, G for UOX, MOX, and GAD FAs; Shaded Box for Reflector)

Fig. 1 17x17 Fuel Assembly and 5x5 Minicore Configuration (Lower Right Quadrant)

3.2 Test Problems

Staring from the 2-D pin cell at uniform temperature to the 3-D mini-core with thermal feedback, there are numerous problems as defined in Table 2. The calculation conditions, problem identifications (ID) and the solution variables of interest are also given in the table. The single character ID's for the thermal condition, C, H, Z, F, D, T, and Q designate cold (300K), hot (600K), hot-zero-power(HZP), hot-full-power(HFP), hot-double-power(HDP), hot-triple- power(HTP), and hot-quadruple-power(HQP), respectively. In the 3-D problems, both top and bottom reflectors which are 20cm thick and consist of water only are added. No shroud is modeled in the radial reflector region in the minicore problem so that the radial reflector also consists of water only.

Table 2 Definition of Test Problems

Geometry	Composition or Configuration	Thermal Condition	Problem Aspects
2-D Pin Cell (PC) with Uniform Temperature	UOX MOX GAD	300K(C) 600K(H)	• Spectrum calculation at cold and hot conditions; Groupwise isotopic cross section data • Regional spectra, eigenvalue
2-D Fuel Assembly (FA) with Uniform Temperature	U M G	300K(C) 600K(H)	• Pin power calculation for different types of FAs; Resonance calculation method • Eigenvalue, pin power distn.
2-D Checkerboard (CB) with Uniform Temperature	U/M U/G	600K(H)	• Spectral interaction between FAs; Ray tracing accuracy • eigenvalue, pin power distn.
2-D Pin Cell (PC) with Heat Conduction	UOX	100(F), 200(D) 300(T), 400(Q) % Power	• Regionwise power calculation with intracell thermal feedback • Fuel temperature distribution, Doppler coefficient
3-D Fuel Assembly (FA) with Power and Flow	U	HZP HFP HDP	• T/H calculation at power generation condition; Feedback effects • Pinwise 3-D power
3-D Minicore (MC) with Power and Flow	5x5 Reflected Core	HZP HFP	• Realistic core calculation with pinwise thermal feedback • Radial and axial pinwise power distn.

4. Comparison of DeCART and MCCARD Results

The test problems defined in Table 2 were solved by both DeCART and MCCARD codes. In addition, the 2-D problems with uniform temperature were solved by the HELIOS code with the most accurate transport and resonance calculation options - the direct collision probability calculation option not requiring any current coupled collision probability calculation and the group-wise multiple resonance category option. Since DeCART uses the

same cross section library (45 Group) as HELIOS, it is expected that the two solutions be close. In the problems with thermal feedback, the MCCARD T/H calculation method was used in DeCART as well to assure consistency in the T/H solution. In order to ensure sufficient accuracy, large numbers of histories were used in the MCCARD calculations (e.g. 100,000 particles x 1000 cycles for the 2-D checkerboard problems) while fine ray tracing options were used in the DeCART calculations (e.g. 0.2 mm ray spacing, and 32 azimuthal and 8 polar angles for the whole 4π solid angle). The flat source regions defined in the DeCART models are shown in Fig. 2. In the following, detailed comparisons are made for each group of problems.

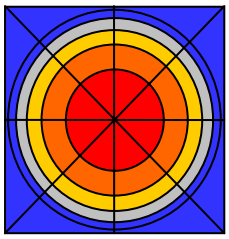

- 3 equivolume rings in pellet
- 1 cladding ring (gray)
- 1 moderator ring (blue) and remaining moderator regions in square
- 8 azimulthal sectors

Fig. 2 Flat Source Regions Defined in a Pin Cell in DeCART Calculations

4.1 2-D Uniform Temperature Problems

The k-effective values obtained for the 2-D uniform temperature cases by MCCARD, DeCART and HELIOS codes are compared in Table 3. As indicated in the table, the k-effective error of DeCART is less than 100 pcm except for a few cases involving the Gadolinia fuel. Note that the error in this table is given in pcm $\Delta\rho$ except for the Gadolinia pin cases whose k-effectives are exceptionally small. The agreement between DeCART and HELIOS is also very good in all the cases excluding the Gadolinia bearing assembly cases with about 106 pcm difference at maximum. This three way comparison thus ensures the soundness of DeCART solutions and also the validity of the HELIOS cross section library data used in these calculations.

Table 3 k-effective Comparison for 2-D Uniform Temperature Problems

Geom.	Fuel Type	Temp K	MCCARD(M)		DeCART(D)		HELIOS(H)		
			k-eff	s.dev pcm	k-eff	D-M pcm	k-eff	H-M pcm	D-H pcm
2D Pin	UOX	300	1.48947	11	1.48777	-77	1.48744	-92	15
		600	1.41203	11	1.41341	69	1.41165	-19	88
	MOX	300	1.26773	13	1.26646	-79	1.26710	-39	-40
		600	1.17095	13	1.17167	52	1.17156	44	8
	GAD	300	0.14240	2	0.14364	124	0.14362	122	2
		600	0.16633	2	0.16743	110	0.16737	104	6
2D FA	U	300	1.50242	7	1.50045	-87	1.50076	-74	-14
		600	1.43859	8	1.43920	30	1.43827	-15	45
	M	300	1.29637	10	1.29462	-104	1.29577	-36	-69
		600	1.20286	9	1.20251	-24	1.20319	23	-47
	G	300	1.36956	9	1.36802	-82	1.36680	-147	65
		600	1.29412	9	1.29540	77	1.29362	-30	106
2D CB	U/G	600	1.36723	6	1.36823	53	1.36750	14	39
	U/M	600	1.31101	6	1.31077	-14	1.31089	-7	-7

The neutron spectra obtained at the outer pellet region in the pin cell problems are compared in Fig. 3. The outer region is the outermost region of the three equivolume regions within the pellet. The 45 group spectra of MCCARD and DeCART obtained for the UOX, MOX, and Gadolinia fuel pins, respectively, coincide almost each other. This excellent agreement in spectrum indicates that the multigroup deterministic transport solutions of DeCART are fully consistent with the continuous energy Monte Carlo solution because the multigroup slowing down and resonance calculation methods perform well and also the cross section data are sound.

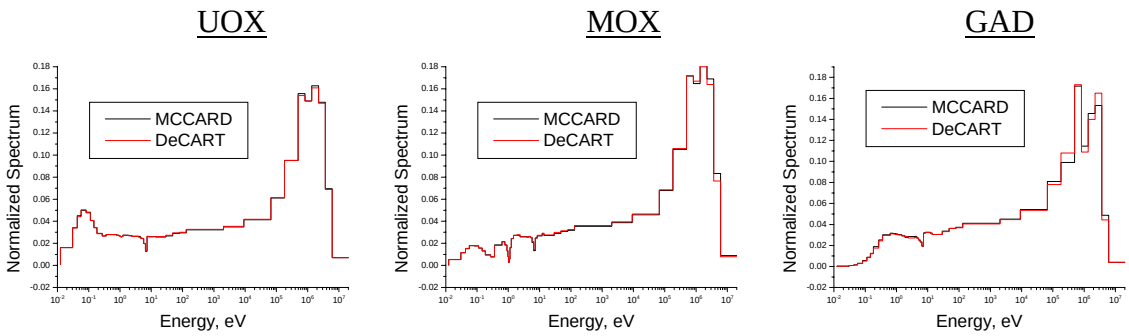

Fig.3 Comparison of MCARD and DeCART Spectra for Three Fuel Compositions at Cold Condition

The accuracy in the pin power calculation is demonstrated in Fig. 4 showing the MCCARD pin power distribution and corresponding pin power errors of the DeCART solution for the UOX/MOX checkerboard case which involves a large power split between the two assemblies. The standard deviation of each pin power is less than 0.1% in the MCCARD calculation. As marked in Fig. 4, the maximum pin error of DeCART is only 0.7%. The pin power error for the assembly cases is even smaller than this. The small pin error assures that the transport solution scheme of DeCART by ray tracing works well.

	1.245 -0.007	1.240 -0.006		1.214 -0.006	1.183 -0.007		1.030 -0.002	0.840 -0.001	1.113 -0.001	0.987 0.004		0.926 0.003	0.918 0.001		0.909 0.002	0.908 0.001	
	1.203 -0.004	1.199 -0.005	1.231 -0.007	1.173 -0.004	1.143 -0.003	1.127 -0.005	0.998 -0.002	0.836 -0.001	1.107 0.001	0.939 0.005	0.944 0.002	0.878 0.005	0.869 0.005	0.914 0.001	0.862 0.004	0.859 0.004	
		1.194 -0.003	1.228 -0.006	1.174 -0.005	1.143 -0.003	1.126 -0.004	0.996 -0.001	0.835 -0.001	1.108 0.000	0.941 0.005	0.948 0.003	0.882 0.006	0.874 0.004	0.918 0.001	0.864 0.004		
				1.215 -0.006	1.189 -0.007		1.025 -0.002	0.836 -0.002	1.108 -0.001	0.991 0.002		0.949 0.002	0.936 0.003				
				1.183 -0.003	1.187 -0.004	1.125 -0.002	0.979 0.001	0.821 -0.001	1.093 0.000	0.937 0.005	0.983 0.005	0.981 0.005	0.927 0.006				
						1.083 -0.003	0.943 -0.003	0.802 0.000	1.072 0.001	0.900 0.003	0.949 0.003						
						0.991 -0.001	0.898 -0.001	0.778 0.001	1.054 0.001	0.886 0.005	0.886 0.005	MCCARD DeCART-MCCARD					
							0.840 0.001	0.749 0.002	1.047 0.001	0.905 0.004							
								0.706 0.003	1.107 0.002								

UOX Side **MOX Side**

Fig. 4 Comparison of Pin Power Distributions for UOX/MOX Checkerboard Problem

4.2 2-D Pin Cell with Heat Conduction

The 2-D pin cell problems with heat conduction are the simplest one among those

involving T/H feedback. These problems were solved by both codes using essentially the same T/H solver. Four problems involving 100% to 400% of the nominal linear power density were solved. In the T/H calculation, 9 rings were used in the pellet region, the coolant temperature was fixed to 290°C, and the mass flow rate was adjusted in proportion to the power level. Fig. 5 illustrates the temperature profile obtained for the 200% case (HDP). In addition to the calculations with the fuel temperature profile within the pellet, the flat fuel temperature cases were also examined in order to address the concern of the fuel temperature profile effect on the Doppler coefficient [6]. In the flat temperature case, the pellet average temperature determined from the corresponding nonuniform temperature case involving thermal feedback calculation was used. The average temperature and reactivity calculated by both code for the 8 cases are listed in Table 4. These results are also plotted in Fig. 6 with the square root of the fuel temperature in Kelvin as the abscissa.

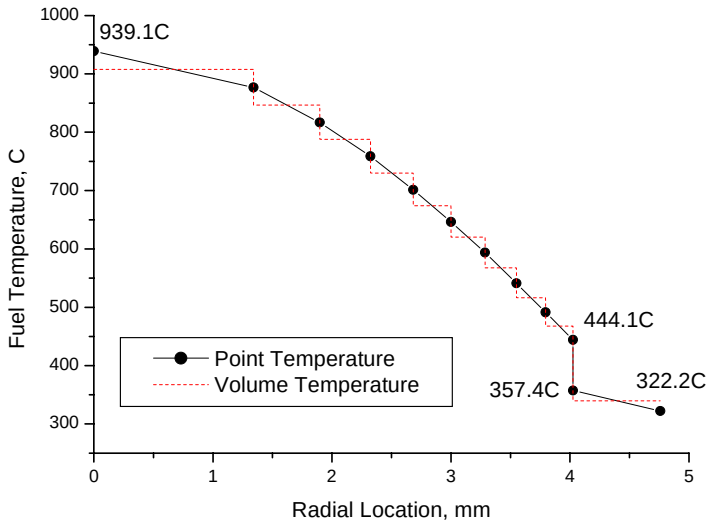

Fig. 5 Calculated Fuel Temperature Profile for a 2-D Pin Cell Problem with Heat Conduction

Table 4 Reactivity and Temperature Obtained for 2-D Pin Cell Problems with Heat Conduction

LHGR kw/m	MCCARD				DeCART				DeCART-MCCARD	
	Avg. Temp.	Reactivity		Profile Effect*	Avg. Temp.	Reactivity		Profile Effect*	Profile*	Flat*
		Profile	Flat			Profile	Flat			
11.0	480	0.29595	0.29578	17	480	0.29573	0.29567	6	-22	-11
21.9	681	0.29266	0.29225	41	680	0.29260	0.29208	53	-6	-17
32.9	912	0.28936	0.28877	59	909	0.28912	0.28833	79	-24	-45
43.9	1167	0.28594	0.28519	75	1168	0.28593	0.28444	150	-1	-76

* in pcm; LHGR=Linear Heat Generation Rate

As shown in Table 4 and Fig. 6, the agreement between MCCARD and DeCART is quite good for the cases with the temperature profile. The DeCART errors are less than 25 pcm. However, for the flat temperature cases, the DeCART error increases with the fuel temperature and thus the reduction slope is steeper in case of DeCART. As a result, the temperature profile effect which causes higher reactivity due to the lower fuel temperature in the peripheral region having higher importance than the flat temperature case appears much larger for DeCART. This behavior is somewhat strange because better agreement is expected

for the flat temperature cases which are easier and simpler problems. It can be explained only by admitting that the temperature dependent resonance integral data are in error for high temperatures, but this error is compensated luckily by the error in the subgroup resonance treatment method for the cases having nonuniform fuel temperature distributions. The impact of the error in the slope on the fuel temperature coefficient (FTC) is shown in Table 5 which leads -0.1 pcm/°C of DeCART for the flat temperature case. Note that the fuel temperature coefficient here was calculated assuming the linear relationship between reactivity and square root of fuel temperature which yields a reciprocal dependence of FTC on the square root of fuel temperature in Kelvin.

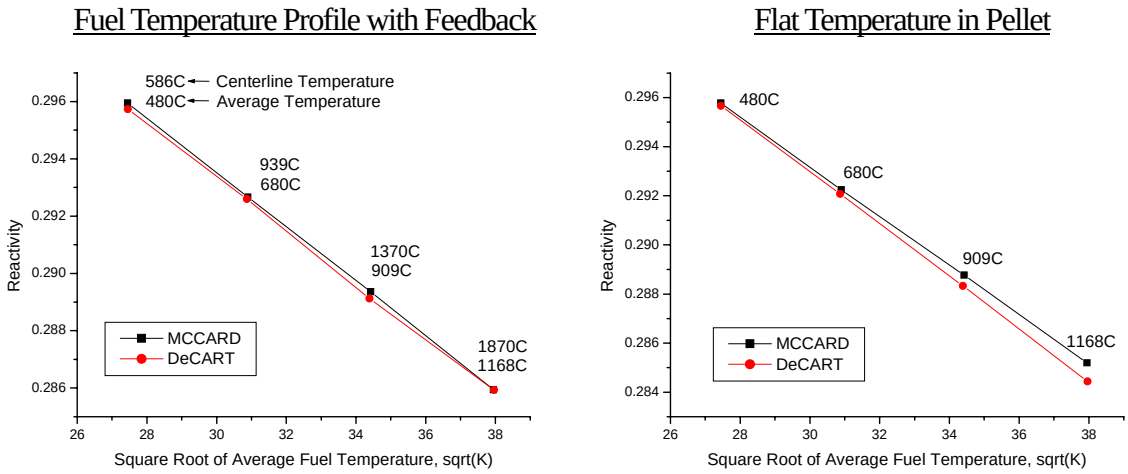

Fig. 6 Reactivity vs. Fuel Temperature for 2-D Pin Cell Problems with Heat Conduction

Table 5 Effect of Temperature Profile on Fuel Temperature Coefficient

Parameter	Profile		Flat	
	MCCARD	DeCART	MCCARD	DeCART
Slope, pcm/sqrt(K)	-95.1	-93.8	-100.6	-106.8
FTC at 1000K	-1.50	-1.48	-1.59	-1.69
FTC Error, pcm/C		0.02		-0.10

4.3 3-D Assembly with Power and Flow

The 3-D assembly cases with power and flow involve the coolant temperature calculation as well as the heat conduction calculation in the fuel pellet. As a result of the coolant temperature rise along the channel, a bottom skewed axial power shape is formed at the HFP state. In order to generate the axial power shape, 10 planes were introduced in the MCCARD tallying. DeCART also used 10 planes in the active core, yielding 20 cm planes for the 2-meter high assembly. In the guide tube channels, a fixed temperature of 290°C was used. The k-effective values obtained for the three 3-D assembly cases are given in Table 6 and the axial and radial power distributions are compared in Fig. 7 and 8.

As indicated in Table 6 and Figs. 7 and 8, the DeCART and MCCARD results match very well. Although the discrepancy is a little larger for the HDP (200% Power) case than the HFP case, it is still negligible. The bottom skewed axial power shape at HFP is well represented by both codes. Particularly, the pin power error of 0.3% is considered excellent. This proves that the pin-wise thermal feedback scheme of DeCART works well.

Table 6 k-effectives of the 3-D Assembly Cases with Power and Flow

State	MCCARD(M)		DeCART(D)	
	k-eff	s.dev pcm	k-eff	D-M pcm
HZP (0.01%)	1.44423	8	1.44405	-9
HFP (100%)	1.42553	8	1.42544	-4
HDP (200%)	1.41830	8	1.41970	70

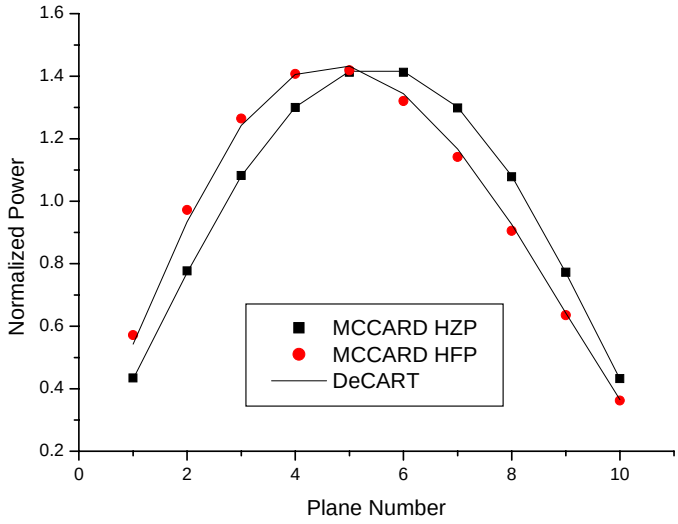

Fig. 7 Comparison of Axial Power Shapes for the 3-D Assembly Case with Power and Flow

1.059 -0.003	1.021 0.000							
1.058 -0.002	1.020 0.000	1.021 0.001						
	1.057 -0.001	1.059 -0.002						
1.054 0.000	1.018 0.000	1.021 0.000	1.066 -0.001	1.048 0.001	MCCARD DeCART-MCCARD			
1.049 -0.001	1.014 0.001	1.017 0.001	1.066 -0.003	1.077 -0.002				
	1.040 -0.001	1.042 -0.001		1.054 0.000	1.028 -0.001	0.967 0.003		
1.017 0.000	0.985 0.000	0.984 0.001	1.016 0.001	0.978 0.001	0.953 0.000	0.929 0.002	0.912 0.002	
0.955 0.000	0.952 -0.001	0.951 0.000	0.952 0.000	0.942 0.000	0.928 0.001	0.914 0.003	0.906 0.001	0.900 0.002

Fig. 8 Comparison of Radial Power Distribution for the 3-D Assembly HFP Case

4.4 Minicores

The 3-D minicore cases are the most realistic problems of the test problem set in that these involve the vacuum boundary and very heterogeneous power distributions. The temperature feedback effect would thus be strongly space dependent. Because of the excessive memory requirement in MCCARD for this large problem, only one mesh was used in the fuel temperature calculation within the fuel pellet and the gap conductance was not modeled. The

same heat conduction model was used in DeCART as well. The primary results obtained for the 3-D HZP and HFP cases are given in Table 7 along with the power and fuel temperature distribution plots in Figs. 9 through 11.

It can be noticed that the power distribution error of DeCART for the HZP case is very small as identified with the RMS error of 0.42% and maximum relative pin power error of 1.8%. The maximum assembly-wise power distribution error is only 0.25% as shown in Fig. 9. This excellent agreement between the MCCARD and DeCART results for the HZP case proves that the transport solver of DeCART is very accurate. Despite the negligible error in the power distribution, the eigenvalue error is somewhat large. The 291 pcm error is the largest error noted in the test problems.

For the HFP problem, larger errors are noted in the power distribution than the HZP case. The maximum pin power error is 3.7% and the DeCART power is higher in the central region than the MCCARD power while it is lower in the peripheral region as shown in Fig. 10. The axial power shapes shown in Fig. 11 coincide very well though whereas the fuel temperature of DeCART is slightly over predicted. The higher fuel temperature of DeCART is a consequence of over-prediction of pin powers in the central region where the power is higher. On the other hand, the eigenvalue error of the HFP case is in the same order as the HZP case. This means that there is no serious additional source of error due to thermal feedback although it causes a slight increase in the power distribution error. The common under prediction of the k-effective by more than 260 pcm in the HZP and HFP cases might be due to the error in the leakage rate in the minicore core involving significant leakages. Further investigation including the treatment of the scattering effect is necessary to identify the exact causes of this problem.

Table 7 Summary of 3-D Minicore Calculation Results

Case	k-eff			Pin Power Error		Fr	
	MCCARD	DeCART	Error pcm	RMS	Max. Rel %	MCCARD	Error %
HZP	1.22526	1.22091	-291	0.42	1.79	2.364	-0.02
HFP	1.19692	1.19317	-263	1.46	3.71	2.041	0.97

HZP

2.088	1.325	0.751
2.089	1.328	0.751
-0.02	-0.25	0.05
DeCART	1.100	0.776
MCCARD	1.098	0.775
D-M, %	0.12	0.11

HFP

1.870	1.266	0.786
1.827	1.255	0.793
2.34	0.87	-0.88
DeCART	1.094	0.819
MCCARD	1.090	0.828
D-M, %	0.32	-1.09

Fig. 9 Comparison of Assembly-wise Power Distributions for Minicore Problems

4.5 Run Time Performance

For the minicore HFP problem, the MCCARD calculation was performed with 100,000 neutrons per cycle and 1000 cycles per T/H calculation in the second stage. During the first

stage, the initial number of active cycles was 100. Five T/H calculations were performed in the first stage yielding a total of 1500 cycles (=100+200+300+400+500) and additional two T/H calculation were performed in the second stage yielding another 2000 cycles. Therefore a total of 3500 cycles of Monte Carlo calculations were performed to lead to a simulation of 0.35 billion histories. The calculation took 48.7 hours on a cluster of thirty-two 1.8 GHz Pentium IV based personal computers. On the other hand, the DeCART calculation required 7 T/H calculations (7 ray tracing calculations as well) for the same problem and the run time was 1.4 hours on a cluster of twenty four 1.8 GHz Pentium IV based personal computers. Therefore, there is roughly a factor of 50 gain in the computation time with the DeCART deterministic calculation over the MCCARD Monte Carlo calculation.

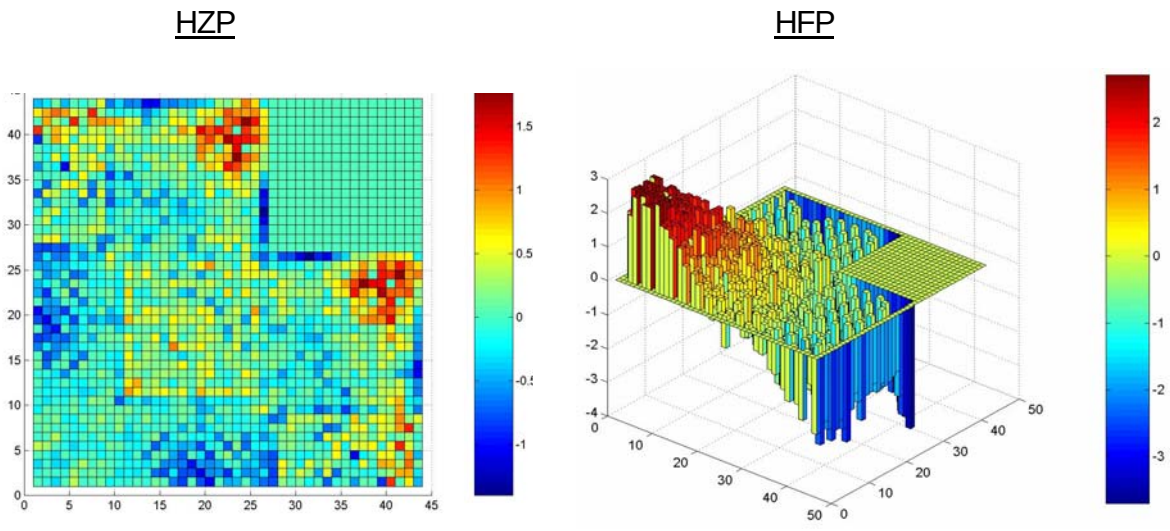

Fig. 10 DeCART Radial Pin Power Distribution Error in Percent for Minicore Problems

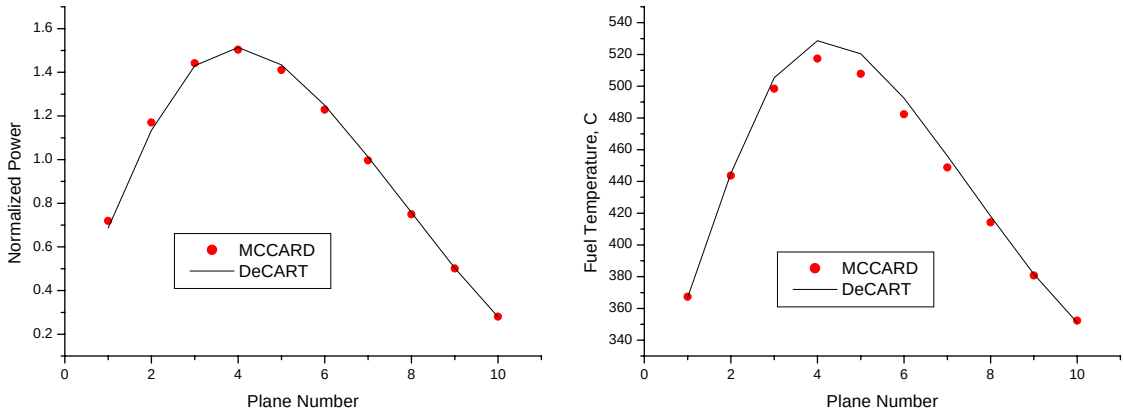

Fig. 11 DeCART Axial Power and Fuel Temperature Distributions

5. Conclusion

By using a suitably designed test problem set, it was possible to perform a systematic and consistent comparison of the continuous energy Monte Carlo solutions and multigroup

whole-core transport solutions for various core states including power generating conditions. The excellent agreement noted for the uniform temperature 2-D and 3-D problems, identified with the nearly identical spectra, the pin power errors less than 1% and the eigenvalue error of 100 pcm in most cases, proves that the transport solver of DeCART performs well and the cross section library data for the nominal operating temperature range are sound. The nonuniform temperature 2-D pin cell problems, however, raises the possibility of error compensation in the resonance treatment at the high temperature range. The worse agreement between MCCARD and DeCART observed for the flat fuel temperature cases than for the cases with a parabolic fuel temperature profile suggests that the resonance integral data and the resonance treatment method for the nonuniform temperature condition need improvements. The consequence of this problem seems to appear in the 3-D minicore HFP case which reveals a overall tilt in the radial pin power error as identified by Fig. 10. The under prediction of the core k-effective by more than 260 pcm for the minicore cases involving large leakages needs further investigation including the treatment of the scattering effect. Nonetheless, the maximum pin power error is only 3.7% and the k-effective error can be regarded small enough. Thus it can be concluded that accurate multigroup direct whole core calculations are possible even at power generating conditions with a much less (a factor of 50) computing time than the corresponding Monte Carlo calculations.

Acknowledgements

This work was supported by the International Nuclear Research Energy Initiative (I-NERI) program jointly funded by the Ministry of Science and Technology of Korea and the Department of Energy of the United States.

References

1) H. G. Joo, et al.. "Methods and Performance of a Three-Dimensional Whole-Core Transport Code DeCART," Proc. PHYSOR2004 – The Physics of Fuel Cycles and Advanced Nuclear Systems: Global Developments, Chicago, Illinois, April 25-29, on CD-ROM, American Nuclear Society, Lagrange Park, IL. (2004).
2) H. J. Shim, B. S. Han, and C. H. Kim, "Numerical Experiment on Variance Biases and Monte Carlo Neutronics Analysis with Thermal Hydraulic Feedback," International Conference on Supercomputing in Nuclear Application, SNA03, Paris, France, Sept. 22-24, 2003, Paper 103, on CD-ROM (2003).
3) R. J. J. Stamm'ler, "HELIOS Methods," Studsvik Scanpower (2002).
4) R. E. MacFarlane et al, "NJOY91.13, A Code System for Producing Pointwise and Multigroup Neutron and Photon Cross Sections from ENDF/B Evaluated Nclear Data," Radiation Shielding Information Center Peripheral Shielding Routine Collection, PSR-171, Oak Ridge National Laboratory (1991).
5) LANL T-2 Nuclear Information Service Home Page, http://t2.lanl.gov/codes/codes.html.
6) K. Smith, Studsvik Scanpower, Inc., Personal Communication, June 18, 2003.